Remote Sensing of Environment 262 (2021) 112487

Contents lists available at ScienceDirect

Remote Sensing of Environment

journal homepage: www.elsevier.com/locate/rse

Persistent upwelling in the Mid-Atlantic Bight detected using gap-filled, high-resolution satellite SST

Sarah C. Murphy [a,*], Laura J. Nazzaro [a], James Simkins [b], Matthew J. Oliver [b], Josh Kohut [a], Michael Crowley [a], Travis N. Miles [a]

[a] Department of Marine and Coastal Sciences, Rutgers, The State University of New Jersey, New Brunswick, NJ, USA
[b] Remote Sensing and Biogeography Group (ORB), University of Delaware, Newark, DE, USA

ARTICLE INFO

Editor: Menghua Wang

Keywords:
Sea surface temperature
GOES-16
Satellite
Upwelling
Mid-Atlantic Bight
Cloud removal
Cold pool
High-resolution

ABSTRACT

This study applied a Spike-Filter (SF) method to identify and remove rapidly moving clouds over the coastal ocean in GOES-16 satellite sea surface temperature fields (SST). These images were then gap-filled to capture upwelling in the Mid Atlantic Bight (MAB), a critical process that impacts ecosystems and atmospheric processes in the region and is important to coastal regions around the world. During the 2019 upwelling season, the default Quality Filter (QF) provided to identify and remove clouds from GOES SST consistently removed upwelling pixels, resulting in ~15% MAB coastal SST coverage. The Spike Filter (SF) method increased MAB coastal SST coverage to 30% and maintained overall accuracy. GOES SF DINEOF SST approximately doubled the number of detected upwelling days compared to MUR SST. The longest upwelling event detected in GOES SF DINEOF persisted for over 17 days, which is longer than upwelling events previously observed in the MAB (Glenn et al., 2004).This suggests that the MAB can have persistent, rather than episodic upwelling as previously thought. Clear detection of the timing and duration of upwelling events is important as it provides estimates for ecological and physical responses in the MAB and coastal regions around the world. GOES-16 SST has the potential to improve upwelling detection and should be further studied for application in ocean and atmospheric modeling.

1. Introduction

Upwelling affects the ecology and dynamics of coastal regions throughout the world (Schwing et al., 1996). The frictional stress of wind on the ocean causes surface water to be transported offshore and be replaced by cold, nutrient rich-bottom waters. The transport of the nutrient-rich bottom waters in the euphotic zone stimulates primary production, drives coastal food webs and sequesters carbon dioxide. Upwelling is responsible for some of the world's most highly productive fishing regions including the coastal waters of Peru and California (Narayan et al., 2010). During the springtime in the Mid Atlantic Bight (MAB), cold remnant winter water is surrounded by the warming surface water, and warmer offshore slope water, creating an isolated area of deep winter water known as the cold pool (Lentz, 2017). Throughout the summer, the cold pool remains along the bottom of the mid shelf. If persistent southerly winds develop, cold bottom water is upwelled to the surface along the coast as the warm surface water is driven offshore (Castelao et al., 2010). During an upwelling event, cold SST can be seen along the coast and extending offshore of recurrent upwelling centers off NJ and the Delaware Bay (Fig. 1). In the MAB, summertime upwelling events are known to produce large coastal blooms and are linked with hypoxic bottom conditions resulting in major financial losses for the shell fishing industry (Glenn et al., 2004). In addition to ecological impacts, upwelling can impact atmospheric processes. By increasing the land-sea thermal gradient, upwelling has been shown to influence sea breeze circulation (Seroka et al., 2018). The occurrence of upwelling and sea breeze in the MAB coincide with electricity demand peaks, making it significant for offshore wind resource assessment. Due to the impact on both the fishing and renewable energy industries, amongst other stakeholders, it is important that upwelling can be readily detected in the MAB.

Upwelling cold water can be identified by measuring sea surface temperature (SST) in coastal regions. Prior to the 1970s, SST measurements were limited to in situ retrieval from buoys, boats, and along shorelines (Minnett et al., 2019). These methods require rigorous sampling and have limited resolutions and coverage. In the MAB, the

* Corresponding author at: Rutgers, The State University of New Jersey, 71 Dudley Road, New Brunswick, NJ 08901-8520, USA.
E-mail address: scm215@marine.rutgers.edu (S.C. Murphy).

https://doi.org/10.1016/j.rse.2021.112487
Received 23 October 2020; Received in revised form 15 March 2021; Accepted 3 May 2021

absence of National Data Buoy Center (NBDC) buoys in the recurrent upwelling centers make it likely that only large upwelling events that extend further offshore are detectable by long-term buoy measurements. Satellite measurement of SST have resulted in major advancements in oceanography and atmospheric sciences. Thermal infrared satellites measure SST by detecting emitted radiation, which varies with temperature (Wentz et al., 2005). Thermal infrared instruments used for measuring SST include Moderate Resolution Imaging Spectroradiometer (MODIS), Advanced Very High Resolution Radiometer (AVHRR), Geostationary Operational Environmental Satellite Imager (GOES), and others. However, satellite measurements can be limited because they are often obscured by clouds, require atmospheric corrections, and have infrequent return periods (Maurer, 2002).

The GOES-16 satellite (GOES), launched on November 19th, 2016, greatly improves the spatial and temporal resolution of previous GOES systems and other available satellites SST products (Schmit et al., 2017). High temporal resolution GOES images have the potential to provide greater SST coverage of coastal regions and small-scale oceanographic processes. GOES provides global SST coverage in hourly composites whereas polar orbiting satellites provide global coverage twice per day, per satellite and can be collected when the satellite is within range of a receiving station. These measurements are important for studying coastal upwelling events, which can evolve over hours to a few days. Upwelling events in the MAB are highly variable in size and duration and have been observed to occur for up to half of the days in the summer season (Glenn et al., 2004). The frequency and variability of coastal upwelling makes it difficult to study without high resolution data, making the newly available hourly GOES satellite technology very valuable.

Despite improvements to satellite SST data by GOES, appropriate detection and removal of clouds is a persistent issue. Data quality control measures designed to remove cloudy pixels from satellite measurements often inadvertently remove cold upwelling water. SST considered good quality by the default data quality flag (QF) developed by NOAA for GOES is effective at removing cloud pixels but has been observed to remove cold coastal ocean pixels throughout upwelling events (Shabanov et al., 2010). This study proposes a technique involving a series of quality control tests and SST reconstruction to closely examine coastal upwelling in the MAB. Having a complete and robust SST dataset is not only important for understanding oceanographic processes, but can also provide insight for coupled ocean-atmosphere phenomena across global and local scales.

2. Methods

The GOES hourly SST product used in this study is derived from observations made by the NASA Geostationary Operational Environmental Satellite 16 (GOES-16) satellite (Mission Overview, 2020). GOES-16 is an advanced geostationary satellite offering high resolution atmospheric, oceanic, solar, and space-weather data via multiple state-of-the-art instruments. After launching in November 2017, GOES-16 underwent multiple calibrations, validations, and testing as it drifted towards its operational location at 89.58° W above the equator. In December 2017, GOES-16 was announced as operational and succeeded GOES-13 to become the GOES-East satellite. The primary instrument aboard the satellite is the Advanced Baseline Imager (ABI) which has 16 spectral bands equipped with the ability to scan full-disk (Western Hemisphere) at 15-min intervals and 0.5–2.0 km spatial resolution. Multiple products have been derived from the ABI bands since the satellite has become operational. The primary product used for this study is SST. The SST product provides key ocean temperature information at full-disk spatial resolution and hourly temporal resolution. GOES SST is archived with NOAA at NCEI and is rapidly accessed in google cloud following data access protocols described here: https://www.ncdc.noaa.gov/data-access/satellite-data/goes-r-series-satellites.

Summary information on the GOES-16 SST product is provided in Table 1. The algorithm responsible for producing GOES-16 SST is the Advanced Clear-Sky Processor for Oceans (ACSPO). The ACSPO requires ABI spectral bands 7 (3.9 μm), 11 (8.5 μm), 13 (10.35 μm), 14 (11.2 μm), and 15 (12.3 μm). These ABI inputs are used in conjunction with

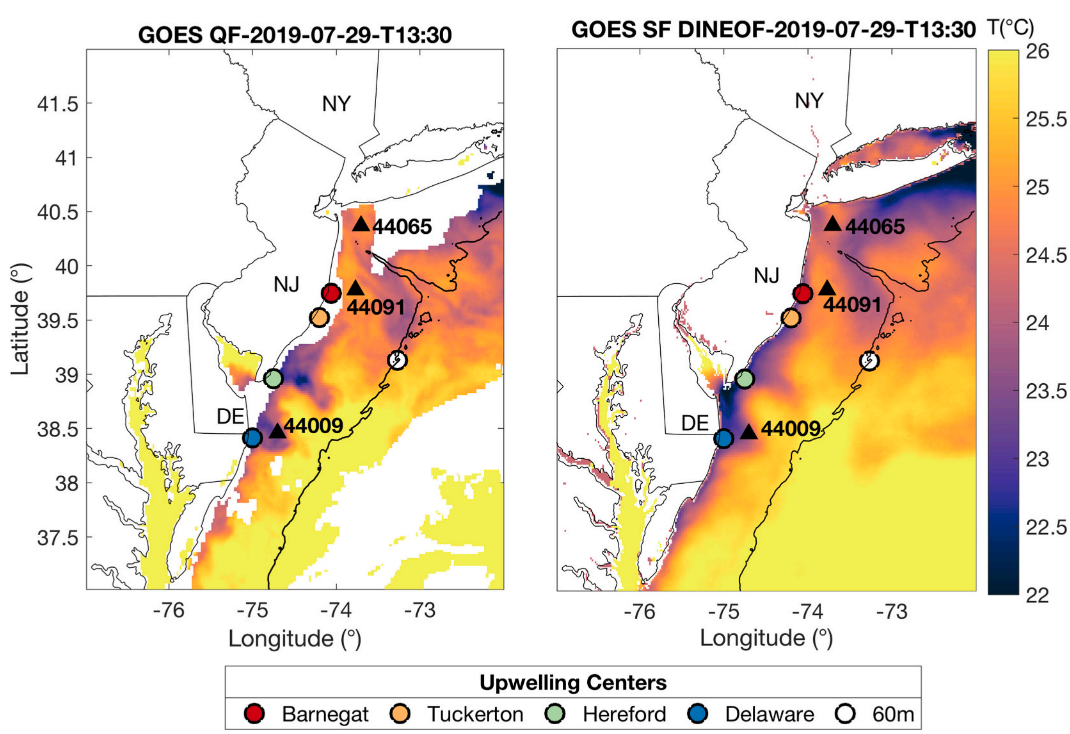

Fig. 1. GOES QF (left) and GOES SF DINEOF reconstructed (right) hourly SST images of the Mid Atlantic Bight study area. Bathymetry contours are drawn for the coastline, and at -60 m offshore. The locations of buoys used for validation (black triangles), the recurrent upwelling centers (colored circles), and the 60 m offshore reference point (white circle) are shown. U.S. state boundaries are outlined and labeled.

Table 1
Satellite SST summary information for SST products used in analysis: MUR, AVHRR, and GOES-16.

	MUR	AVHRR	GOES-16
Satellite	observations from several instruments and climatology	Polar-Orbiting	Geostationary
Source	GHRSST L4	GHRSST L3C	L2+
Coverage	Global	Global	−77°W to −72°W 37°N to 42°N
Spatial Resolution	0.01 degrees (Latitude) x 0.01 degrees (Longitude)	0.05 degrees × 0.05 degrees	0.5–2.0 km
Temporal Resolution	Daily	Twice Daily	Hourly
Processing	GDS version 2	Multispectral algorithm and bias correction	ACSPO
Target Accuracy	<0.4 K	<.4 K	1 K
Time Span	2002-Jun-01 to Present	2016-Jan-06 to Present	2017-Dec-15 to Present
Platform/ Sensor	Aqua/AMSR-E Aqua/ MODIS InSitu/InSitu, NOAA-19/AVHRR-3 Terra/ MODIS CORIOLIS/WINDSAT GCOM-W1/AMSR2	MetOp-B/AVHRR-3	GOES-16/ABI

ancillary global weather data, ancillary Reynold's SST fields, ABI cloud and ice masks, and ABI clear-sky brightness temperatures to create the SST data. Extensive quality control is performed on each pixel of SST data which involves significant validation comparisons to existing operational SST products and in situ buoy observations. The output includes multiple variables which include SST and Data Quality Flags (DQF) for each pixel.

The data is uploaded in near-real-time to a publicly accessible Google Bucket. The University of Delaware Ocean Exploration, Remote Sensing and Biogeography Laboratory (ORB Lab) extracts the GOES-16 SST data in real-time via this Google Bucket and performs a reprojection of the spatial dataset at 2.0 km resolution, which they make publicly available on the ORB Lab databases at: *http://basin.ceoe.udel.edu/thredds/* (Simkins, 2019). In this study, SST from the ORB lab database is extracted for the Mid Atlantic Bight within −77°W to −72°W and 37°N to 42°N.

3. Spike filter

The GOES ABI processing system uses a preliminary cloud masking and subsequent Quality Control (QC) test to determine usable cloud-free ocean pixels for SST retrieval (Ignatov, 2010). First, the ABI Cloud Mask identifies cloudy pixels which are not considered for use by the SST algorithm and is designed to minimize the discarding of potential good data. Next, the remaining pixels, which may still have significant cloud contamination, are annotated by the Data Quality Flags (DQF) into four categories: "Good," "Degraded," "Severely Degraded." And "Poor." The QC tests observed Brightness Temperature (BTs) for consistency with the Community Radiative Transfer Model (CRTM) which uses Ancillary Global Forecast System and Optimal Interpolation SST data as input (Mission Overview). SST flagged as "Optimal" by the DQF was retained for the GOES Quality Filtered SST. This strategy of separate preliminary cloud masking and subsequent data quality flags suggests the development of individual quality control products. Because cold coastal upwelling SST pixels are often removed by global quality flagging methods in the Mid Atlantic Bight (Glenn et al., 2004) the Spike Filter (SF) method was designed to retain coastal upwelling SST pixels and applied to un-flagged GOES hourly SST.

The SF method is designed to further quality control SST by detecting sudden changes in temperature due to the presence of clouds, which typically persist for shorter time periods than coastal upwelling. The National Buoy Data Center (NBDC) quality control measures use similar time continuity and range limit checks to filter out rapid changes in ocean temperature and are described in further detail in the NBDC Technical Document 09–02 (NBDC, 2009). The SF method includes the following four sequential steps: 1. Rate of SST change 2. Minimum SST threshold 3. Comparison to recent SST 4. SST bias correction. First, for each SST pixel, any change in temperature per pixel greater than 1 °C/ hour was removed, as surface ocean cooling rates are highly unlikely to exceed this threshold. Glider observations demonstrated that during a strong hurricane event, the surface ocean cooled at a rate of 0.5 degrees per hour in this region (Glenn et al., 2016) representing a likely upper bound for cooling from ocean processes. Next, any SST below 12 °C was removed. SST is not expected to decrease below 12 °C in this region in the summer upwelling season. A climatology study which used 150 years of observations found the mean monthly SST value for the MAB from June–September to be 18–23 °C (Richaud et al., 2016). In addition, upwelling studies observed a minimum SST of ~16°C along the coast of New Jersey (Glenn et al., 2004) and in the Delaware Bay (Voynova et al., 2013) during upwelling events. Next, any data more than 2 standard deviations outside a moving 7 day per pixel average was removed. Lastly, the bias correction was applied to GOES SST that had passed the previous three steps of the SF method. Bias corrections in satellite SSTs are typically derived from in situ SSTs to produce a more accurate estimate of SST at the depth of the buoys (Reynolds et al., 2002; Downing and Williams, 1975). The bias calculation applied in this study was created so that it could be applied to upwelling-retained GOES SF SST. Bias was calculated as the difference between buoy SST and GOES SST matched to the buoy locations and times of measurement averaged over the upwelling season, June 1–September 20. These values were calculated at NBDC buoys 44025, 44089, 44091, 44009, and 44065 and then averaged for the entire time period. This analysis included additional buoys outside of the coastal upwelling zone to provide an accurate interpolation across the domain. The averaged biases were: 44089: 0.1502, 44025: 0.2884, 44065: 0.2090, 44009: 0.3461, and 44091: −0.0198 °C. These values were placed in the GOES spatial domain at each of the corresponding buoy locations and then interpolated across the entire domain using inverse distance weighting interpolation (Fig. 2). The interpolated grid of bias values was then added at every GOES SST pixel for the entire time period.

3.1. DINEOF gap-fill

The GOES SF SST was then reconstructed using Data Interpolating Empirical Orthogonal Functions (DINEOF) (Alvera-Azcárate et al., 2005). Validation studies of DINEOF used for oceanographic data sets demonstrate robust results containing realistic and reliable ocean features. DINEOF is a technique that calculates missing data from an optimal number of Empirical Orthogonal Functions (EOF) obtained by cross-validation. This analysis ensures that the reduced variables represent a large fraction of the original variability of the data (Alvera-Azcárate et al., 2005). In the DINEOF algorithm, the temporal and spatial average of the original dataset is removed and the first EOF mode is calculated using Singular Value Decomposition to estimate the missing data. This process is repeated until convergence is obtained for the estimated values for each EOF mode for the desired maximum number of modes. Once the optimal number of EOF modes are determined, the reconstruction is performed again for those modes.

The DINEOF method was performed on the SST dataset which contained 276 × 278 pixels and 2315 hourly images. Final spatial size after excluding land points was 34,876 pixels and contained an average of 66.29% missing data. DINEOF reconstruction was performed using the entire data set with a maximum of 20 EOF modes computed. The reconstruction parameter was set so that DINEOF reconstructed the entire matrix using the EOF base to avoid cold spikes at cloud edges and

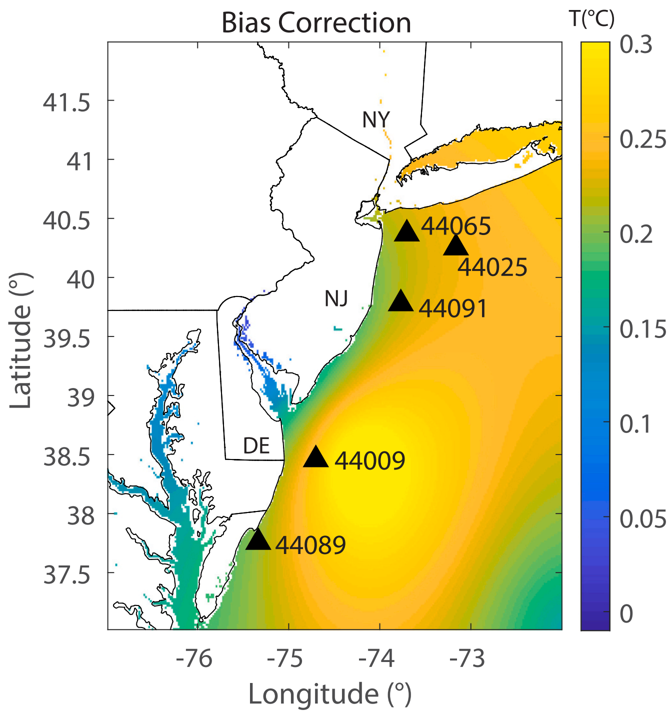

Fig. 2. Bias correction applied to GOES SF based on averaged bias of GOES compared to buoy SSTs for the summer time period using Inverse Distanced Weighted Interpolation. Buoys used to calculate GOES SF SST bias are shown as black triangles.

other sources of noise in the original matrix. The covariance matrix was filtered prior to reconstruction using an alpha value of 0.01 (the strength of the filter) and a Numit value of 1500 (the reach of the filter), selected to filter frequencies higher than 24 hours out of the data set. The Numit value was fine-tuned, similar to the methods used by Alvera-Azcárate et al. (2009) and 1500 was determined to provide the most accurate reconstruction while retaining the upwelling signal. The reconstructed GOES SST was validated at every stage of the methods against NBDC buoy SST. Buoys located in the MAB and inshore of the 30 m isobath were chosen for validation to focus on known upwelling regions. These included 44065 (New York harbor entrance, 40.369 N 73.703 W) 44009 (southeast of Cape May, 38.457 N 74.702 W), and 44091 (Barnegat, 39.778 N 73.769 W). The root mean square (RMS) error: satellite minus buoy, model bias: mean satellite minus mean buoy, CRMS: (satellite minus mean satellite) minus (buoy minus mean buoy), and total count: number of data available for comparison.

4. Results

4.1. Satellite observations

Hourly GOES SF DINEOF improved SST coverage of the Mid-Atlantic Bight for the time period studied when compared to twice daily composited AVHRR and daily MUR SST by providing more SST measurements at a high resolution and acceptable accuracy (see Table 1 for SST product details; see Table 2 for validation statistics). MUR is a global product that provides daily SST images created from observations from several instruments at 0.01° latitude x. 01° longitude resolution. The AVHRR product chosen for analysis in this study is a global product that provides twice daily composited images from its polar-orbiting satellite passes at 0.05° latitude x 0.05° longitude resolution. These products were chosen because they are readily accessible global SST products that demonstrate the current ability of both satellite SST and gap-filled SST to detect upwelling in the MAB. As shown in Fig. 3, GOES better captures the complexity of ocean features in the region, while AVHRR SST is coarser and the shape of the coastal upwelling water is less defined. MUR SST appears to smooth the details of ocean features as well as underestimate the coldness of the upwelling SST. In the GOES Spike Filtered image, which is used for the GOES SF DINEOF reconstruction, both the offshore extent of upwelling and near shore pixels are well defined. GOES-16 also has a higher temporal resolution and contains hourly images as opposed to the twice daily composited AVHRR product and daily composited MUR product. GOES SF DINEOF provides ~17 times the number of AVHRR and MUR SST pixels for each buoy (Fig. 5, Table 2). The GOES SF DINEOF SST has a comparable RMS error to the MUR filled in product and significantly lower RMS error than AVHRR.

4.2. GOES inter-product comparisons

As an example, Fig. 3 compares how various SST products capture an upwelling event on July 27, 2019. The GOES Quality Filtered image is missing most of the cold SST off the southern tip of NJ and the Delaware Bay (Fig. 3). The GOES default quality filter consistently flagged upwelling SST pixels as severely degraded throughout upwelling events observed in this study. Upwelling SST was also missing from AVHRR and MUR SST collected the same day, unlike the data filtered using the SF method. The SF method effectively identified and removed cloudy data offshore while retaining coastal upwelling SST pixels in the Delaware Bay region. When applied to the entire time period, the SF improved coverage in the critical upwelling zone along the coast of New Jersey and Delaware (Fig. 4). Coverage was calculated as the number of timestamps per pixel containing SST data out of the total images in the studied time period. GOES QF SST provided low coverage along the coast, with SST measurements ~15% percent of the summer. GOES SF SST increased coverage in the coastal region to ~30% and was comparable to the percent coverage in the surrounding area offshore.

GOES, AVHRR, and MUR SST were validated for accuracy against regional NBDC buoy SST measurements 44065, 44009, and 44091, which were located nearest to the upwelling centers off NJ and DE, and is presented in Fig. 5 and as summary statistics in Table 2. Buoy SST were provided at varying temporal resolutions of 10-min (44065), 30-min (44091) and hourly (44009) data. GOES Quality Filtered (QF), GOES Spike Filtered (SF) and GOES SF DINEOF SST was extracted at the location of each buoy and compared to the nearest in time buoy SST measurement. The SST extracted from all three GOES data sets accurately match the overall trends in SST observed at buoy 44091 (Fig. 5). GOES SST data contains early summer warming and late summer

Table 2
Summary of SST validation statistics. Validation performed at NBDC buoys 44009, 44091, and 44065 for GOES QF, GOES SF, GOES SF DINEOF, AVHRR, and MUR. The GOES SF DINEOF SST is validated to a 24-hour smoothed buoy SST.

	44091					44009					44065				
	GOES QF	GOES SF	GOES SF DINEOF	AVHRR	MUR	GOES QF	GOES SF	GOES SF DINEOF	AVHRR	MUR	GOES QF	GOES SF	GOES SF DINEOF	AVHRR	MUR
RMS:	0.446	0.585	0.63	1.37	0.447	0.802	0.506	0.995	1.8	1.124	0.89	0.845	0.7086	1.42	0.675
CRMS:	0.441	0.535	0.56	1.26	0.445	0.716	0.499	0.985	1.72	0.943	0.80	0.845	0.7027	1.38	0.620
MB:	0.065	−0.237	−0.295	−0.54	0.047	0.37	0.083	−0.141	−0.53	0.611	0.39	−0.012	−0.092	−0.38	0.267
Count:	805	812	2314	135	111	737	843	2314	135	111	681	735	2315	122	111

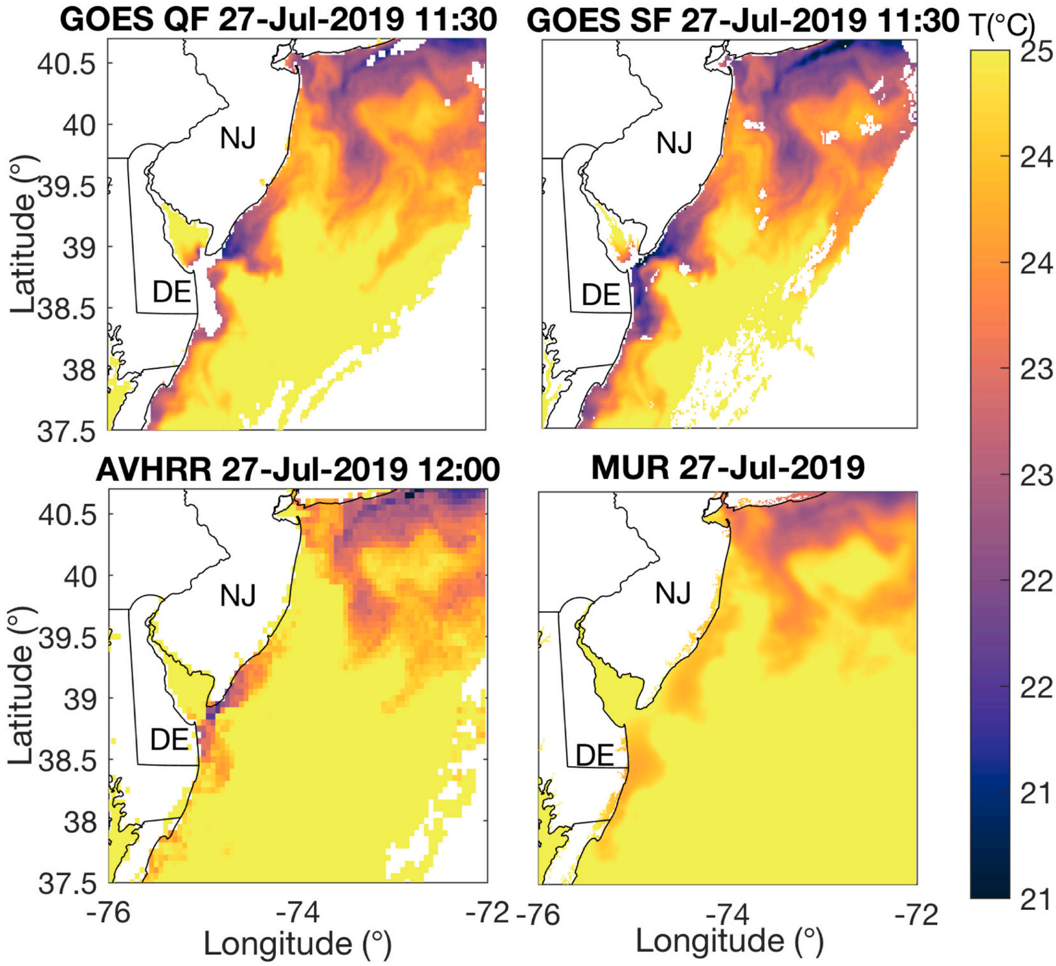

Fig. 3. SST during an upwelling event on July 27, 2019 from the various SST products used for analysis. Images are shown on the top row: GOES QF and GOES SF and on the bottom row: AVHRR, and MUR.

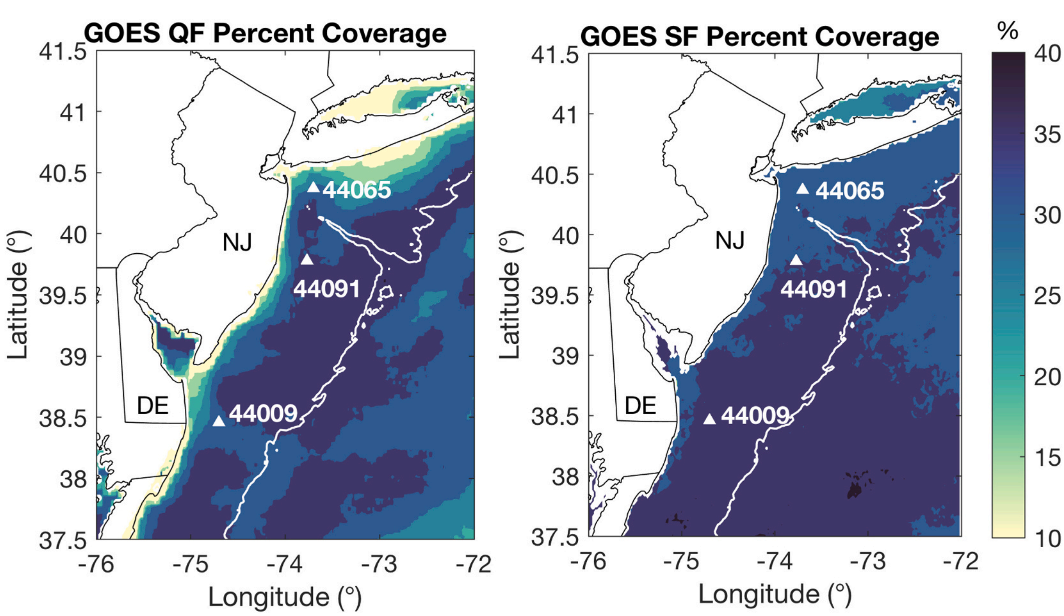

Fig. 4. Percent of SST (non-NaN) data available per pixel for the summer time period (June 1–September 20, 2019) for GOES QF (left) and GOES SF (right).

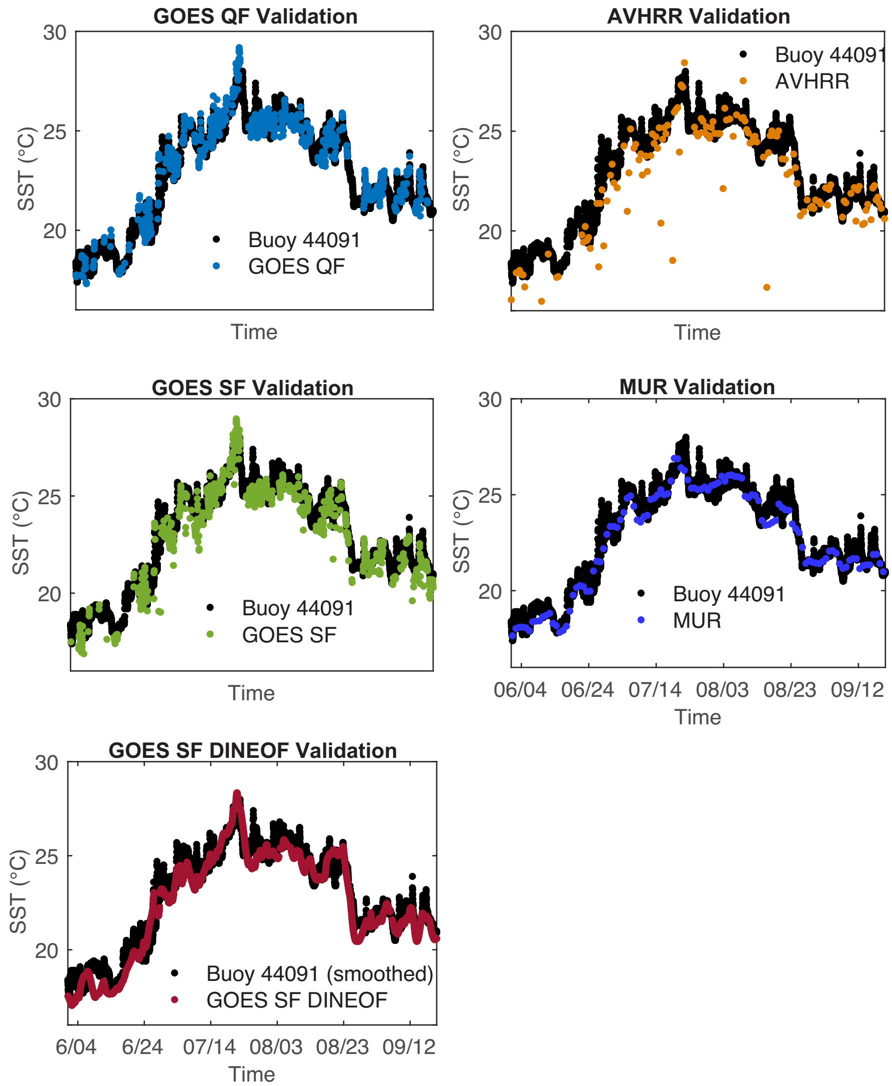

Fig. 5. Validation of GOES SST data sets, AVHRR, and MUR at Buoy 44091 for the summer time period. On the left side, GOES SST (colored dots): QF (Top), SF (Middle) and SF DINEOF (Bottom); On the right side, AVHRR (Top) and MUR (middle); Buoy 44091 SST (black dots) are shown on each panel. GOES SF DINEOF is validated against a 24-hour smoothed buoy SST.

cooling observed by the buoy. In addition, the high quantity of GOES SST measurements detail smaller processes like diurnal cycles. The SF method is less restrictive than the QF and occasionally allows in SST pixels that are colder than the buoy SST observed. However, the SF maintains the accuracy of GOES and GOES SF has a lower average RMS error than GOES QF. GOES SF has a higher RMS error at buoy 44091 where it exceeds QF RMS only by 0.14 of a degree, well within the 1-degree target accuracy of GOES SST. The SF filter preserved more data than the QF filter at each of the three buoys even though all three buoys are located outside of the coastal upwelling zone where the most drastic improvement in coverage was displayed (Fig. 4). Buoy 44009 was the most likely to include upwelled water (Fig. 1) and also had the greatest improvement in both coverage and RMS using the SF method. The bias correction applied to GOES SF SST reduced the warm bias from 0.2090 to −0.012 at buoy 44065 and from 0.3461 to 0.083 at buoy 44009 (Table 2). The SF filter improved coverage of the upwelling zone and maintained accuracy for the limited time period studied.

Sufficient SST coverage in the upwelling zone is important to ensure the accuracy of the DINEOF reconstruction. DINEOF reconstruction of GOES SF SST provided a complete hourly SST data set for the MAB 2019 summer. DINEOF is an EOF based technique that was used in this study to fill in missing SST data likely caused by the presence of clouds. The use of the 24-hour filter and the smoothing function allowed for the upwelling signal to be retained while remaining cloud edges were reduced (Alvera-Azcárate et al., 2009). Despite the gaps in GOES SF SST data, the DINEOF reconstructed GOES SST is accurate to buoy 44009 (Fig. 5, Table 2). For example, around August 23, GOES SF DINEOF SST closely matches the SST observed at buoy 44091 despite a lack of GOES SF SST data at this location and time. GOES SF DINEOF SST contains 2315 measurements at each pixel which more than doubles the number of GOES SF measurements.

4.3. Detecting upwelling

Coastal upwelling was determined by a 2 °C or more difference between inshore and offshore SST, as defined by Glenn et al. (2004). The inshore SST was extracted at the location of 4 recurrent upwelling centers and the offshore SST was extracted at a mid-shelf location, as indicated by the colored circles in Fig. 1. Fig. 6 includes a time series of the differences between inshore and offshore SST for hourly GOES SF DINEOF SST and daily MUR SST. Hourly GOES SST differences that exceeded the 2 °C threshold for a minimum of 24 hours were then

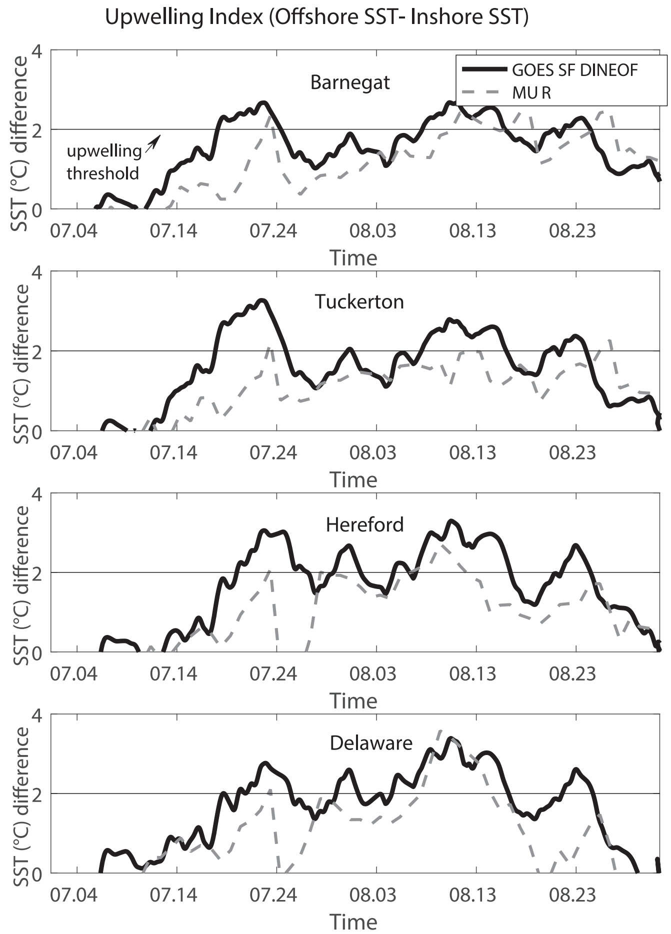

Fig. 6. SST difference (offshore SST – inshore SST) at the 4 upwelling centers in the MAB for the summer time period. GOES SF DINEOF SST hourly SST differences (solid lines) and GHRSST MUR SST daily SST differences (dashed lines) are shown. The upwelling threshold is defined as an SST difference in 2 °C or greater.

Table 3
Upwelling detection results from GOES SF DINEOF and MUR for June 1–September 20, 2019. Results calculated for the days detected as upwelling by each product- GOES SF DINEOF (33 days) and MUR (15 days). Upwelling days for GOES SF DINEOF were designated as any day when more than half the hourly passes for that day exceeded the upwelling threshold.

	GOES SF DINEOF	MUR
Total Upwelling Days	33	15
Percent of summer upwelling occurred	30%	13.5%
Average upwelling SST	22.5 °C	22.97 °C
Minimum upwelling SST	17.1 °C	17.88 °C
Maximum SST Diff (Off-Inshore)	3.4 °C	3.58 °C
Average Duration	6.5 days	3 days
Max Duration	17.66 days	7 days
Average Area Upwelling	3223 km^2	3091 km^2
Max Extent Area	5996 km^2	5799 km^2

summarized into upwelling days for comparison to MUR in Table 3. The beginning and ending of an upwelling event was characterized by the persistence or lack of a 2 °C or colder coastal SST for a minimum of 24 hours. The detection of upwelling is only compared between GOES SF DINEOF and MUR SST because they are both gap-filled datasets. In addition, SST data from GHRSST L3C AVHRR was infrequent at the 4 upwelling centers and contained corrupted cloudy data, so it was not useful for comparisons using this threshold.

During the upwelling season studied, June 1–September 20th, three upwelling events were detected in GOES SF DINEOF SST between July 17th and August 24th, 2019, totaling 33 days or roughly 30% of the summer (Fig. 6, Table 3). The average duration of an upwelling event was 6.5 days and the longest event persisted for 17.66 days. Only 15 total days of upwelling were detected via MUR SST, with an average duration of 3 days and the longest event lasting 7 days. The occurrence of upwelling events detected via GOES SF DINEOF is physically confirmed by the presence of persistent, upwelling-favorable winds, primarily from the southwest at buoy 44009. Winds at buoy 44009 were categorized as upwelling winds 18 hours earlier than SST indicated upwelling, accounting for the local lag between wind and Ekman transport. Winds that occurred during non-upwelling times appeared to be uniformly distributed across different directions.

The average inshore upwelling SST at the 4 upwelling centers observed by both GOES SF DINEOF and MUR was ~22.7 °C and the minimum upwelling SST was ~17.5 °C. Only half of the days of upwelling detected by GOES SF DINEOF were detected via MUR. Fig. 7 shows the median SST of each pixel averaged over the total upwelling events observed by GOES SF DINEOF and MUR. The median upwelling SST for GOES SF DINEOF contained colder SST pixels closest to shore, ~22 °C, that are not present in MUR. In addition to the increased number of upwelling observations, GOES SF DINEOF provided more upwelling pixels per event as indicated by the larger total area of upwelling (Fig. 8). Upwelling pixels were measured as the total number of SST pixels above the upwelling threshold per SST image. GOES SF DINEOF provided a detailed account of the spatial extent of upwelling with a maximum upwelling area of 4410.9 km^2. The maximum area of upwelling observed via MUR was 3128.3 km^2. Because MUR is a blended product that provides full spatial coverage of the MAB, the difference in upwelling area per event was not due to missing data.

Without coastal SST from satellites during upwelling events, MUR is prone to estimating warmer SST in this area, causing fewer days to exceed the upwelling threshold. MUR generally agrees with GOES SF DINEOF in the timing of changes in the inshore-offshore SST difference for the four upwelling centers, but underestimates the value of this difference (Fig. 6) and defines upwelling centers to be warmer and more spatially uniform (Fig. 7). When upwelling is detected by MUR, MUR and GOES SF DINEOF agree on the total area of upwelling (Fig. 8), reinforcing the accuracy of the GOES Spike Filter and DINEOF reconstruction methods. However, for more than half of the time upwelling is detected by GOES, MUR estimates the area of upwelling to be close to zero. The increase in upwelling pixels retained via the Spike Filter method is helpful in improving the accuracy of GOES SF DINEOF reconstruction.

5. Discussion

Coastal upwelling is a regional ocean phenomenon that is ecologically and physically important to the MAB. Given the dynamic nature of upwelling and the limitations to satellite derived SST, the methods introduced in this study provide novel insight into the spatial and temporal evolution of upwelling events. Upwelling has been observed in the Mid Atlantic Bight in previous studies (Glenn et al., 2004; Seroka et al., 2018; Kohut et al., 2004) using AVHRR SST. AVHRR SST provides less continuous viewing at equivalent or higher spatial resolution compared to GOES-16. Due to the lower temporal resolution, the presence of clouds can cause large gaps in time between available SST from AVHRR. These gaps in measurements make it difficult to accurately characterize the duration of upwelling events.

The total number of upwelling days observed using GOES SF DINEOF in this study falls within the average range previously observed by a study of upwelling in the region using AVHRR (Glenn et al., 2004). However, the longest upwelling event observed in this study using GOES SF DINEOF is longer than the maximum outlier observed previously over 9 years of AVHRR measurements. In Glenn et al. (2004), the average observed lifetime of an upwelling event was ~1 week, and the largest

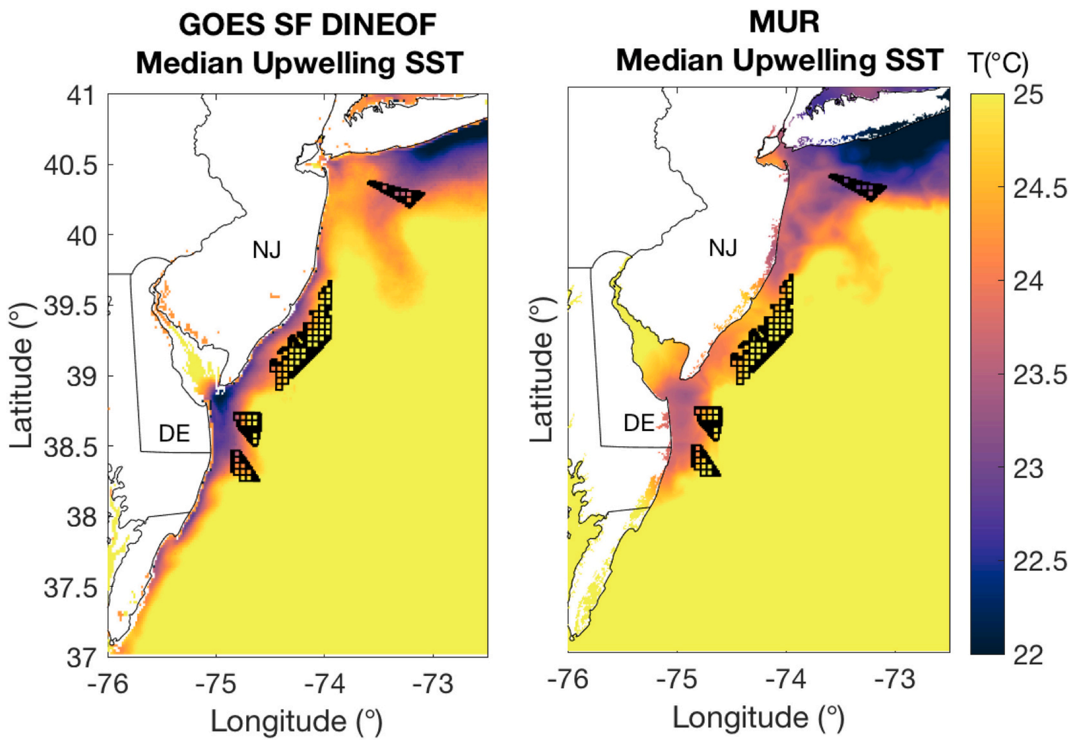

Fig. 7. The median upwelling SST averaged per pixel for the detected upwelling days for GOES SF DINEOF (33 days) AND MUR (15 days). The black shaded polygons illustrate the offshore wind lease areas.

outlier lasted approximately 2 weeks. In this study, the longest upwelling event persisted for over 17 days. The number of events observed in this study, ~3, is also on the lower range of the number of events per summer previously observed (3–8). This suggests that upwelling may be occurring more persistently, rather than a series of short episodic events as previously thought, due to improved detection via a more continuous SST data set.

Coastal upwelling events that were both wind-driven and influenced by tidal mixing were observed in this study along the New Jersey (NJ) coast and the Delaware (DE) Bay. Southerly winds are predominant in the summertime, a driver of coastal upwelling along the New Jersey shelf (Kohut et al., 2004) and consistent with the timing of upwelling events observed during this study. The onset and termination of upwelling events detected using GOES SF DINEOF were more distinct and separated by non-upwelling for longer at the two northern upwelling centers (Barnegat and Tuckerton), while upwelling persisted longer at the two southern sites (Hereford and Delaware). For example, the largest upwelling events persisted for 17.66 days at Hereford and for 11 days at Delaware during the first half of August, while the longest upwelling event at Barnegat and Tuckerton occurred earlier in the season around mid-July. In the beginning of the summer season, notably for the first upwelling event, coastal SST is ~1 °C colder at the two northern sites. Heading into late July/early August, coastal SST was slightly colder at the two southern sites by ~0.5–1 °C, possibly due to the seasonal evolution of the cold pool- the source of the upwelled water; the cold pool warms at a rate of ~1 °C/month but this rate varies and is stronger over Georges Bank and the New York (NY) Bight than it is in the southern Mid Atlantic Bight (Lentz, 2017). In addition, the longer persistence of upwelling events in Delaware Bay is consistent with previous observations and may be influenced by tidal mixing (Voynova et al., 2013). Münchow et al. (1992) suggested that near the Delaware Bay, tidal currents are strong and likely enhance and extend the presence of cold water from upwelling. Voynova et al. (2013), also describe the presence of a shallow canyon and that may allow for a more pronounced Ekman spiral to develop.

Another limitation to satellite SST products is that quality filtering algorithms frequently characterize cold coastal upwelling SST as corrupted data. While an algorithm has been developed to retain upwelling pixels for AVHRR SST in the MAB (Glenn et al., 2016), this algorithm is locally focused with region-specific thresholds, and dependent on channels that are not provided by all sensors. Therefore, this algorithm has not yet been applied to GOES SST and is not applied to global products like GHRSST L3C AVHRR or MUR SST. The Spike Filter method developed in this study for GOES is also specific to the ocean conditions of the MAB and is not a global solution. The Spike Filter is rudimentary and more permissive than the quality filter developed for GOES and may allow for the presence of corrupted cloudy pixels. In addition, the methods used in this study are limited in that they cannot be applied to a single image. They require a time series of SST measurements.

SST from GHRSST L3C AVHRR at the 4 upwelling centers was infrequent and contained corrupted cloudy data, so it was not useful for the characterization of upwelling events using the SST difference threshold. Due to the quality filtering applied to satellite SST products, it is likely that near-coast upwelling SST pixels are not assimilated into the MUR product. Less than half the number of total upwelling days observed using GOES SF DINEOF were observed in MUR SST. The link between upwelling and the MAB ecology is well documented, and accurate detection of the upwelling occurrence is important for ocean and atmospheric modeling as well as for fisheries operations and management in the Mid Atlantic.

The occurrence of upwelling events is modulated by wind forcing, the location of the Cold Pool, the strength of coastal river plumes, and the occurrence of downwelling favorable winds during summer storms (Glenn et al., 2004). Strong downwelling wind events can push cold bottom water farther offshore resulting in less active upwelling. Heavy spring and summer precipitation can increase the strength of the Hudson River plume resulting in a southward jet of low-salinity water and decreasing upwelling activity. Storm frequency can also disrupt upwelling by mixing nearshore waters.

Upwelling transports nutrient-enriched subsurface waters along the

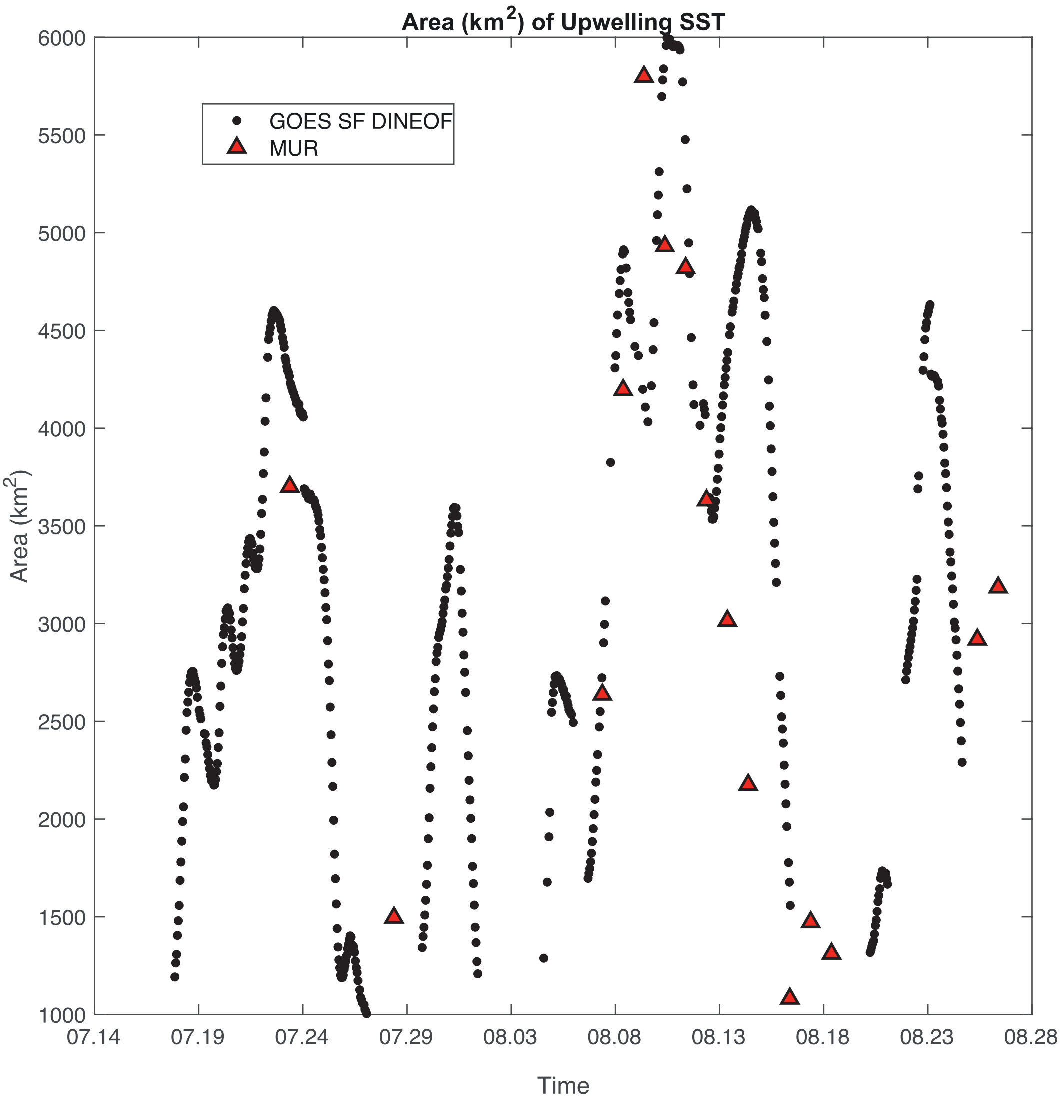

Fig. 8. The total area (km^2) of upwelling SST pixels as detected by GOES SF DINEOF (black circles) and MUR (red triangles) during the upwelling time period. (For interpretation of the references to colour in this figure legend, the reader is referred to the web version of this article.)

New Jersey coast, causing an enhancement of particulate organic carbon and stimulating phytoplankton growth (Glenn et al., 2004). Organic material is distributed offshore into the upwelling center, spreading at the thermocline, and can deplete 75% of the oxygen in the bottom water off the coast of NJ as it is respired at depth. According to Glenn et al. (2004), increased phytoplankton concentrations occur immediately upon the onset of upwelling conditions and the total number of upwelling days provides an estimate of the amount of time that the enhanced organic material is deposited in the upwelling center. Similar effects have been seen in Delaware Bay upwelling events (Voynova et al., 2013). These findings reinforce the importance of clear detection of the timing and duration of upwelling events, which can cause major financial loss for fisheries. Satellite data, along with other observations, is integrated into ocean models in the Mid-Atlantic to support products that have been shown to improve habitat models (Oliver et al., 2013). In the Mid Atlantic coastal ocean, SST and chlorophyll-a fronts, along with other hydrographic processes, influence habitat associations for several species (Manderson et al., 2011). For example, in Oliver et al. (2013), Atlantic sturgeon were observed in shallow, well-mixed, warm freshwater associated with a Delaware Bay water mass. Knowing the timing and location of this endangered species can inform management recommendations to reduce interactions with fisheries.

Coastal upwelling has also been shown to impact the offshore component of sea breeze circulation (Seroka et al., 2018), the timing of which is critical to the offshore wind industry. Offshore wind operations will rely on accurate wind forecasting to match electricity demands. Filaments of upwelling were observed to extend entirely through portions of the NJ wind energy area and were present in the shoreward half during most of the upwelling events. The location of the current wind energy areas in the MAB are shown in Fig. 7 as shaded polygons. Upwelling SST frequently occupied the entirety of the offshore wind leased areas off Delaware and Long Island. Seroka et al., 2018, simulated the impacts of upwelling on sea breeze circulation using a maximum averaged upwelling SST from AVHRR imagery. As demonstrated in this study, upwelling events are extremely dynamic and may be occurring more frequently, and for longer durations than can be detected by lower resolution products like AVHRR and MUR. An operational, daily gap-filled image derived from Spike-Filtered GOES SST dataset is likely to provide significant improvements to the detection of upwelling. This is indicated in Table 3 which degrades the detection of upwelling via hourly GOES passes into total upwelling days. However, the hourly resolution of GOES SST was preserved for potential future applications that could benefit from sub-daily SST variability. For example, using high resolution GOES SST as input in atmospheric modeling may provide further insight into the effects of upwelling on sea breezes in the Mid Atlantic.

6. Conclusion

This study demonstrates the value of GOES hourly SST in improving observations of coastal upwelling in the Mid Atlantic Bight. When compared to global SST products like AVHRR and MUR, GOES provides 2000 additional SST measurements at regional buoy locations over the peak upwelling season and detects more than twice the number of upwelling days. The default GOES quality filter frequently removes cold upwelling pixels which has been previously identified as a problem for quality filtering in many satellite SST sources. We use a Spike Filter method to retain coastal upwelling in GOES SST. These upwelling centers are likely not included in standard AVHRR or MUR SST composites. The SF method aided in maintaining the accuracy of GOES SST DINEOF gap-filled composites in the coastal zone. This study demonstrates the importance of developing an operational quality filtering algorithm for GOES SST that retains upwelling pixels so that it can be readily used to improve observations of coastal upwelling in the Mid Atlantic Bight. An improved bias correction technique should also be developed that can be applied to upwelling retained in GOES SST.

Coastal upwelling is a unique feature that must be accurately represented in terms of temperature, frequency, and duration because of its importance to the ecology and physics of the region. Previous studies have used AVHRR imagery which has lower temporal resolution and can be significantly obscured by clouds. The use of GOES hourly SST to observe upwelling has suggested that upwelling events may be more persistent than previously thought. Future climatology studies of upwelling in the MAB should use cloud-free upwelling retained GOES SST to accurately characterize the temporal and spatial evolution of coastal upwelling and the unique physical conditions of the Mid Atlantic Bight. Improvements to the characterization of upwelling are especially useful to the fishing and renewable energy industries. Upwelling events have been linked with hypoxic bottom conditions off the NJ coast (Glenn et al., 2004) and delivery of subsurface nutrients that support phytoplankton primary production to the lower Delaware Bay (Voynova et al., 2013). Upwelling has also been shown to influence sea breeze circulation and is a research interest of the offshore wind industry (Seroka et al., 2018). Atmospheric modeling studies should be conducted using hourly updating GOES SST to provide realistic ocean conditions and determine the impact of SST fields on wind forecasting.

Upwelling occurs in many coastal regions including off the coast of California, Northwest and Southwest Africa, Chile, and Peru (Summerhayes, 2014). The methods developed in this study could be adjusted and applied in these regions as local cloud detection and removal techniques are needed to retain coastal upwelling pixels in satellite SST images and DINEOF can be readily used to gap-fill SST images. The failure of MUR to detect up to half of the upwelling events observed using GOES SF DINEOF in the MAB suggests that the use of previously available SST products may have limited the detection of upwelling events. These methods may help in broadening our understanding of the ecosystem and atmospheric impacts of upwelling in coastal regions around the world.

Funding

This work was supported by the Department of Marine and Coastal Sciences, Rutgers University, New Brunswick, NJ, USA.

Research data

The methods and data used in this study to identify and remove clouds and gap-fill GOES-16 hourly SST are linked here: Murphy, Sarah (2020), “GOES-16 SST: cloud correction and gap filled for observation of upwelling in the MAB”, Mendeley Data, V1, doi: 10.17632/npnfntz3kp.1

The original GOES-16 SST can be accessed here: http://basin.ceoe.udel.edu/thredds/dodsC/GOESNOAASST.nc.html

CRediT authorship contribution statement

Sarah Murphy: Conceptualization, Data curation, Formal analysis, Investigation, Methodology, Validation, Visualization, Writing - original draft, Writing - review & editing. **Laura Nazzaro:** Data curation, Investigation, Methodology, Resources, Software, Writing - review & editing. **James Simkins:** Data curation, Resources, Software, Validation, Visualization, Writing - review & editing. **Matthew Oliver:** Conceptualization, Investigation, Methodology, Writing - review & editing. **Josh Kohut:** Conceptualization, Investigation, Methodology, Writing - review & editing. **Michael Crowley:** Data curation, Validation. **Travis Miles:** Conceptualization, Investigation, Methodology, Funding acquisition, Project administration, Supervision, Writing - review & editing.

Declaration of Competing Interest

The authors declare that they have no known competing financial interests or personal relationships that could have appeared to influence the work reported in this paper. This work was supported by the Department of Marine and Coastal Sciences, Rutgers University, New Brunswick, NJ, USA.

References

Alvera-Azcárate, A., Barth, A., Rixen, M., Beckers, J.M., 2005. Reconstruction of incomplete oceanographic data sets using empirical orthogonal functions: application to the Adriatic Sea surface temperature. Ocean Model 9 (4), 325–346. https://doi.org/10.1016/j.ocemod.2004.08.001.

Alvera-Azcárate, A., Barth, A., Sirjacobs, D., Beckers, J.-M., 2009. Enhancing temporal correlations in EOF expansions for the reconstruction of missing data using DINEOF. Ocean Sci. 5, 475–485. https://doi.org/10.5194/os-5-475-2009.

Castelao, R., Glenn, S., Schofield, O., 2010. Temperature, salinity and density variability in the central middle Atlantic bight. J. Goephys. Res. 115 https://doi.org/10.1029/2009JC006082.

Downing, H.D., Williams, D., 1975. Optical constants of water in the infrared. J. Geophys. Res. 80 (12), 1656–1661. https://doi.org/10.1029/JC080i012p01656.

Glenn, S., et al., 2004. Biogeochemical impact of summertime coastal upwelling on the New Jersey Shelf. J. Geophys. Res. 109 https://doi.org/10.1029/2003JC002265. C12S02.

Glenn, S., Miles, T., Seroka, G., Xu, Y., Forney, R., Yu, F., et al., 2016. Stratified coastal ocean interactions with tropical cyclones. Nat. Commun. 7 https://doi.org/10.1038/ncomms10887.

Ignatov, A., 2010. Advanced Baseline Imager (ABI) Algorithm Theoretical Basis Document for Sea Surface Temperature (NOAA NESDIS STAR).

Kohut, J.T., Glenn, S.M., Chant, R.J., 2004. Seasonal current variability on the New Jersey inner shelf. J. Geophys. Res. 109 https://doi.org/10.1029/2003JC001963. C07S07.

Lentz, S.J., 2017. Seasonal warming of the middle Atlantic bight cold Pool. J. Geophys. Res. Oceans 122, 941–954. https://doi.org/10.1002/2016JC012201.

Manderson, J., Palamara, L., Kohut, J., Oliver, M., 2011. Ocean observatory data are useful for regional habitat modeling of species with different vertical habitat preferences. Mar. Ecol. Progr. 438, 1–17. https://doi.org/10.3354/meps09308.

Maurer, J., 2002. Infrared and Microwave Remote Sensing of Sea Surface Temperature. University of Hawaii, Department of Aerospace Engineering Sciences. http://www2.hawaii.edu/~jmaurer/sst/ (accessed 1 June 2020).

Minnett, P.J., et al., 2019. Half a century of satellite remote sensing of sea-surface temperature. Remote Sens. Environ. 233, 111366. https://doi.org/10.1016/j.rse.2019.111366.

Mission Overview, 2020. https://www.goes-r.gov/mission/mission.html (accessed 8, March, 2020).

Münchow, A., Masse, A.K., Garvine, R.W., 1992. Astronomical and nonlinear tidal currents in a coupled estuary shelf system. Cont. Shelf Res. 12 (4), 471–498.

Narayan, N., Paul, A., Mulitza, S., Schulz, M., 2010. Trends in coastal upwelling intensity during the late 20th century. Ocean Sci. 6 (3), 815–823. https://doi.org/10.5194/os-6-815-2010.

NBDC, 2009. Handbook of Automated Data Quality Control Checks and Procedures. NBDC Technical Document 09–02.

Oliver, M., Breece, M., Fox, D., Haulsee, D., Kohut, J., Manderson, J., Savoy, T., 2013. Shrinking the haystack: using an AUV in an Integrated Ocean observatory to map atlantic sturgeon in the Coastal Ocean. Fisheries 38 (5), 210–216. https://doi.org/10.1080/03632415.2013.782861.

Reynolds, R., Rayner, N., Smith, T., Stokes, D., Wang, W., 2002. An improved in situ and satellite SST analysis for climate. J. Clim. 15, 1609–1625. https://doi.org/10.1175/1520-0442(2002)015<1609:AIISAS>2.0.CO;2.

Richaud, B., Kwon, Y., Joyce, T.M., Fratantoni, P.S., Lentz, S., 2016. Surface and bottom temperature and salinity climatology along the continental shelf off the Canadian and U.S. East Coasts. Cont. Shelf Res. 124, 165–181. https://doi.org/10.1016/j.csr.2016.06.005.

Schmit, T.J., Griffith, P., Gunshor, M.M., Daniels, J.M., Goodman, S.J., Lebair, W.J., 2017. A closer look at the ABI on the GOES-R series. Bull. Am. Meteor. Soc. 98, 681–698. https://doi.org/10.1175/BAMS-D-15-00230.1.

Schwing, F.B., O'Farrell, M., Steger, J.M., Baltz, K., 1996. Coastal Upwelling Indices — West Coast of North America. NOAA, Technical Memorandum, 1946–95, NMFS NOAA-TM-NMFS-SWFSC-231.

Seroka, G., Fredj, E., Kohut, J., Dunk, R., Miles, T., Glenn, S., 2018. Sea breeze sensitivity to coastal upwelling and synoptic flow using Lagrangian methods. J. Geophys. Res.-Atmos. 123, 9443–9461. https://doi.org/10.1029/2018JD028940.

Shabanov, N., Ignatov, A., Petrenko, B., Kihai, Y., Heidinger, A., 2010. Towards integrated cloud mask and quality control for ABI SST product: prototyping with MSG/SEVIRI. In: 6th Annual Symp. NPOESS&GOES-R, 90-th AMS Annual Meeting, 17-21 January, Atlanta, GA.

Simkins, J., 2019. GOES16 SST Product, Reprojected to EPSG: 4326. University of Delaware Ocean Exploration, Remote Sensing and Biogeography Group (ORB). http://basin.ceoe.udel.edu/thredds/dodsC/GOESNOAASST.nc.html.

Summerhayes, C., 2014. Upwelling. In: Harff, J., Meschede, M., Peterson, S., Thiede, J. (Eds.), Encyclopedia of Marine Geosciences. Springer, Dordrecht. https://doi.org/10.1007/978-94-007-6644-0_96-1.

Voynova, Y.G., Oliver, M.J., Sharp, J.H., 2013. Wind to zooplankton: ecosystem-wide influence of seasonal wind-driven upwelling in and around the Delaware Bay. J. Geophys Res. Oceans 118, 6437–6450. https://doi.org/10.1002/2013JC008793.

Wentz, F., Gentemann, C., Smith, D., Chelton, D., 2005. Satellite measurements of sea surface temperature through clouds. Science 288 (5467), 847–850.